JOURNAL OF MATERIALS SCIENCE 35 (2000) 5421–5425

Ferroelectric and dielectric properties of ferroelectromagnet $Pb(Fe_{1/2}Nb_{1/2})O_3$ ceramics and thin films

X. S. GAO, X. Y. CHEN, J. YIN, J. WU, Z. G. LIU
National Laboratory of Solid State Microstructures, Nanjing University, Nanjing 210093, People's Republic of China
E-mail: zgliu@nju.edu.cn

M. WANG
National Laboratory of Crystal Materials, Shandong University, Jinan, 250100, People's Republic of China

The ferroelectric and dielectric properties of ferroelectromagnet $Pb(Fe_{1/2}Nb_{1/2})O_3$ (PFN) ceramics and thin films prepared by pulsed laser deposition (PLD) have been investigated systematically. PFN ceramics experienced a para-ferroelectric transition and a para-antiferromagnetic transition at 380 K and 145 K, respectively. At room temperature, it has an electrical remnant polarization of 11.5 $\mu C/cm^2$ and a coercive field of 4.04 kV/cm. The dielectric behaviors show characteristics of diffusive phase transition at a wide temperature range around 380 K. Anomalies in the dielectric constant and loss tangent have been observed near the Neel temperature of 145 K, indicating a coupling between the ferroelectric and antiferromagnetic orders in PFN ceramics. At room temperature, the PFN films exhibited a remnant electric polarization of 7.4 $\mu C/cm^2$, a coercive field of 10.5 kV/cm, and a dielectric constant of 486 at frequency of 10 kHz, indicating their potential applications in memory devices.

1. Intruduction

Lead based complex perovskite ferroelectric compound $Pb(Fe_{1/2}Nb_{1/2})O_3$ (PFN) was first discovered by Smolenskii *et al.* [1]. Generally, perovskite-like (ABO_3) compounds have large internal field that is necessary for the appearance of ferroelectric state. At the same time, the angles between the connecting lines "cation B-oxygen-B′" are equal to 180°, forming an optimum condition to the existence of magnetic ordering due to the indirect exchange interaction. In PFN, the electric order is favored by Pb^{2+} in site A and Nb^{5+} in site B. On the other hand, Fe^{3+} in the octahedral site B provides magnetic moment needed for the existence of magnetic order. These are the basis of coexistence of ferroelctric order and ferromagnetic order in this compound. PFN undergoes a ferroelectric phase transition at about 380 K and an antiferromagnetic phase transition at about 145 K [1, 2]. As a result, it becomes a ferroelectromagnet below 145 K. It is well known that spontaneous polarization associated with ferroelectricity is caused by lattice distortion and magnetic ordering is determined by the exchange interaction between electron spins. In ferroelectromagnets the change in electrical ordering caused by ferroelectric phase transition or external electrical field will lead to a redistribution of the electron spins and change its magnetic property. On the other hand, the change in magnetic ordering caused by ferromagnetic phase transition or magnetic field will also lead to the change in ferroelectric and dielectric behavior of the material via a magnetorestritive effect or other electron-phonon interaction mechanisms. The study on the coupling between electrical and magnetic ordering may give us an insight into the mechanism of ferroelctricity and magnetism in this complex perovskite, which may have some possible applications in new type of devices. In addition, PFN is a relaxor ferrolectric having high dielectric constant [3, 4]. Its large spontaneous polarization also makes it a potential material in non-volatile memory applications. In this paper, we report the ferroelectric and dielectric properties of both the ceramics and thin films of PFN.

2. Experimental

The bulk ceramic samples of PFN were prepared by conventional solid state reaction. Stoichiometrical PbO (2 at% excess), Fe_2O_3, and Nb_2O_5 were mixed by ball milling for 12 h, then compacted and calcined in air at 850°C for 2 h. After calcination the products were grounded by ball milling again for 12 h. Finally, the powder was pressed into pellets and sintered at 1050°C for 1 h. The structures of PFN ceramics were examined by X-ray θ-2θ Scan patterns, which shows a single phase. The ceramic samples were then cut and polished for the measurement of ferroelectric and electric properties. Silver paste was used in both surfaces of

specimens as electrodes. The PFN films were grown on Si(001) and $La_{0.7}Sr_{0.3}MnO_3$ coated Si(001) substrate by pulsed laser deposition (PLD). PLD apparatus used in this work has been described previously [5]. Briefly, the output from a KrF excimer laser (LPX 205i, Lambda Physik, 248 nm in wavelength, 30 nm in pulse width) with a beam fluency of about 2.5–3 J/cm^2 and a repetition rate 3 Hz was used. The pressure of flowing ambient oxygen was 20 Pa. In order to measure electrical properties, $La_{0.7}Sr_{0.3}MnO_3$ (LSMO) film was deposited at 700°C as bottom electrodes and Pt as top electrodes. After the deposition, the films were *in situ* annealed in the chamber at 600°C for 30 min. The PFN films were characterized by X-ray θ-2θ Scan patterns using Cu K_α radiation. The morphology of film surface was examined by Scanning Electrode Microscopy (SEM). Transmission Electron Microscopy (TEM) was used to examine the structure of the ceramic samples. The *P*-*E* hysteresis loops of PFN bulk samples and thin films were measured by RT6000 tester (in a Virtual ground mode). Dielectric constant measurements were carried out by an impedance analyzer (YHP4192) in a temperature range of 300 K–420 K and in a frequency range of 1 kHz–1 m Hz. Leakage current was measured by an electrometer (HP4140B, PA meter/DC).

3. Results and discussions

3.1. PFN ceramic samples

Fig. 1 shows the *P*-*E* hysteresis loop of PFN ceramics, showing the remnant polarization and the corresponding coercive field are 11.5 μC/cm^2 and 4.04 kV/cm, respectively. The temperature dependence of dielectric constant and dissipation factor of PFN ceramics at various frequencies are plotted in Fig. 2a and b. At low frequency, a broad peak can be found at about 380 K, in agreement with the Curie temperature of PFN [3, 4]. Dielectric behaviors of PFN ceramics exhibit typical characteristics of diffuse transition. The peak temperature of dielectric constant increases with the increase of the frequency, and the peak temperature of the dissipation factor increases with the decrease of the frequency.

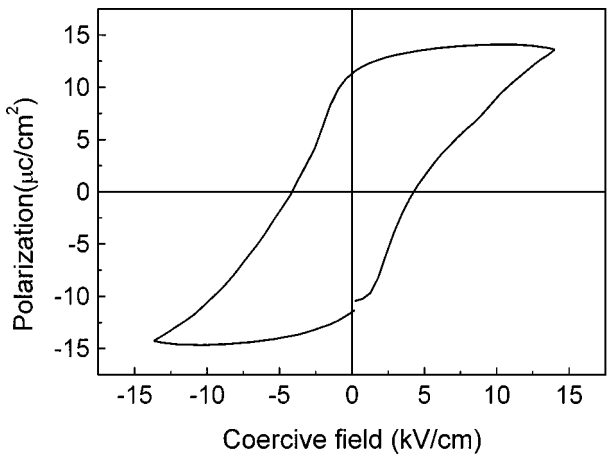

Figure 1 The *P*-*E* hysteresis loop of the PFN ceramic sample. (at an maximum applied voltage of 400 V, Pr = 11.5 μC/cm^2, Ec = 4.04 kV/cm).

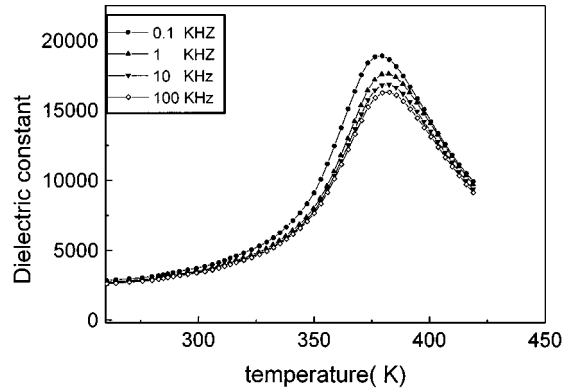

(a)

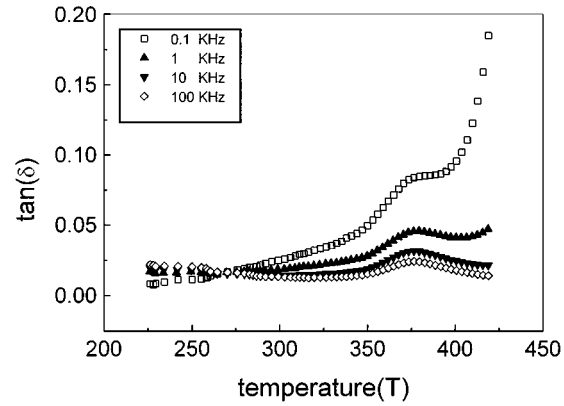

(b)

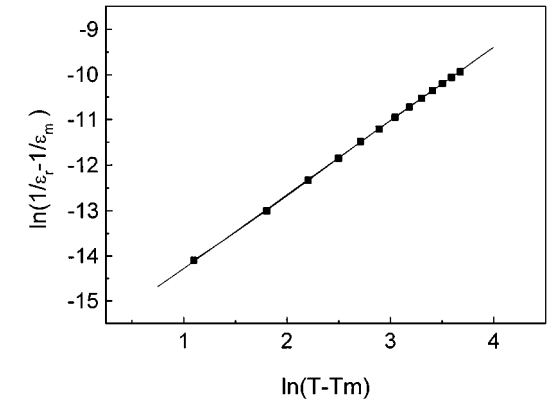

(c)

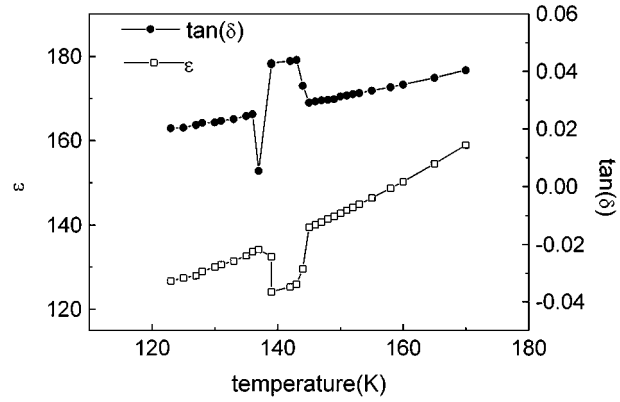

(d)

Figure 2 (a) The temperature dependence of the real part of dielectric constant of PFN ceramic samples. (b) The temperature dependence of the dissipation factor of PFN ceramic samples. (c) ln $(\frac{1}{\varepsilon_T} - \frac{1}{\varepsilon_m})$. vs. ln$(T - T_m)$ at temperature higher than T_m of PFN ceramic samples. (d) The temperature dependence of dielectric constant and the dissipation factor in a region of 120 K–170 K of PFN ceramic samples.

According to the theory of diffuse phase transition in the case of paraelectric phase, the dielectric behaviors are governed by $\frac{1}{\varepsilon_T} - \frac{1}{\varepsilon_m} = c(T - T_m)^\alpha$ [6], where ε_m represents the maximum value of dielectric constant, ε_T the dielectric constant at temperature of T, T_m the temperature of maximum value of dielectric constant peak, c a temperature independent function, and α the diffusive exponent indicating the degree of diffusion. Fig. 2c shows the logarithmic of $(\frac{1}{\varepsilon_T} - \frac{1}{\varepsilon_m})$ against logarithmic $T - T_m$ of bulk ceramics at the temperature higher than T_m. It is obvious that the curve well fits the diffusive equation, and the values of α and lnC estimated by least square methods are 1.62 and –15.9, respectively. The diffusive characteristics can be ascribed to the random distribution of Fe^{3+} and Nb^{5+}, which leads to the fluctuation of the composition, thus forming many microscopic regions with different curie temperatures. It is just these microscopic regions that broaden the transition temperature into a wide temperature region [7]. The occupation of Fe^{3+} and Nb^{5+} in the site B was examined by Transmission Electron Microscopy (TEM). Fig. 3 shows the select area electron diffraction (SAD) patterns of PFN ceramics. The (1/2, 1/2, 1/2) superlattice reflection plots which indicate the ordering of the occupation of ions in site B could not be found, thus confirming that Fe^{3+} and Nb^{5+} are randomly distributed on site B.

To examine the coupling of the magnetic order and the electrical polarization, the dielectric constant and the dissipation factor at 120 K–170 K are measured and presented in Fig. 2d. An anomaly can be observed in both the dielectric constant and the dissipation factor of ceramic samples at about 145 K (the antiferroelectric transition point). The dielectric anomalies in electromagnets have ever been studied by Scott *et al.* [8, 9]. They introduced a magnetoelectric effect free energy term with a form of P^2M^2 to analyze the dielectric anomalies, where P is the spontaneous polarization, M is the sublattice magnetization. In this case, The dielectric anomaly can be explained by magnetorestrictive effect caused by the antiferromagnetic transition. The magnetorestritive effect changes the electrical polarization, thus resulting in the anomaly. Similar anomalies were also observed in the ferroelectromagnetic $YMnO_3$ by Chu *et al.* [10].

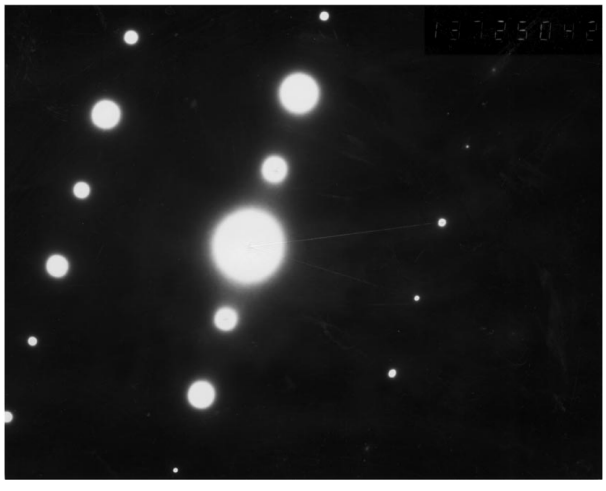

Figure 3 The select area electron diffraction (SAD) patterns of the PFN ceramic samples (showing the random distribution of Fe^{3+} and Nb^{5+}).

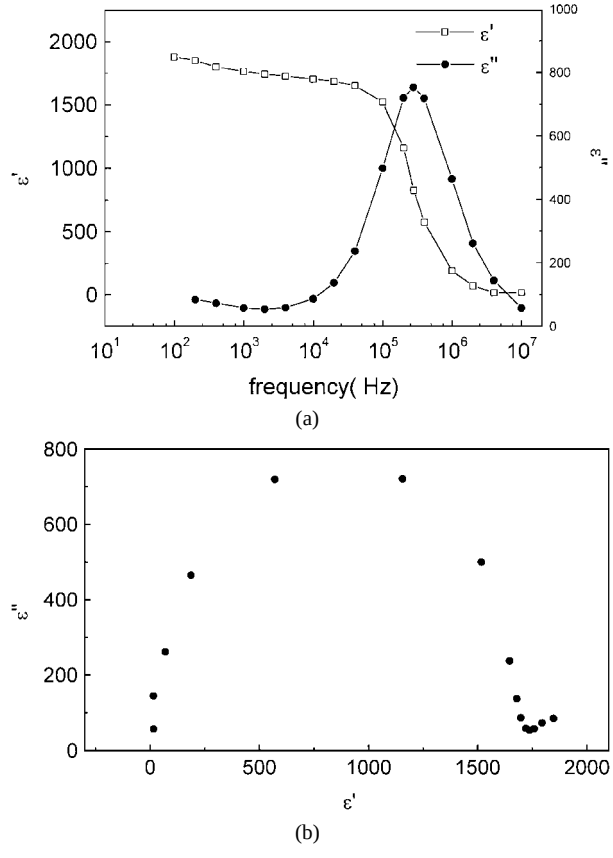

Figure 4 (a) The dielectric spectra of the PFN ceramic sample. (b) Cole-Cole plots of the PFN ceramic samples.

Fig. 4a shows the dielectric spectra of PFN bulk samples. The real part of the dielectric constant of PFN ceramics decrease monotonically with the increase of the frequency and the curve of the imaginary part has a peak at 2.8×10^5 Hz. The dielectric behaviors show the characteristics of the dielectric relaxation with a corresponding relaxation time of 3.2×10^{-6} s. Cole-Cole plots of the ceramic samples are drawn in Fig. 4b. The Cole-Cole plots of bulk samples approximate to a semicircle. This indicates that the bulk samples have a single relaxation time [11], which may be due to the electrode polarization caused by the hopping of iron and oxygen vacancies [12].

3.2. PFN thin films

Fig. 5 shows the XRD patterns of PFN films deposited at 720°C. We found that perovskite phase can be formed only within a narrow substrate temperature range of 700–740°C, outside which pyrochlore phase appears. Fig. 6 shows the SEM surface morphology of PFN films indicating that the surface of PFN film is smooth, dense, and crack free. The average grain size of the PFN film is about 80 nm.

The hysteresis loop of the PFN thin films is shown in Fig. 7, which exhibits good saturation of polarization when the applied voltage is larger than 10 V. The remnant polarization and corresponding coercive field of PFN films are determined to be 7.4 $\mu C/cm^2$, and 10.5 kV/cm, respectively. In contrast to the ceramic

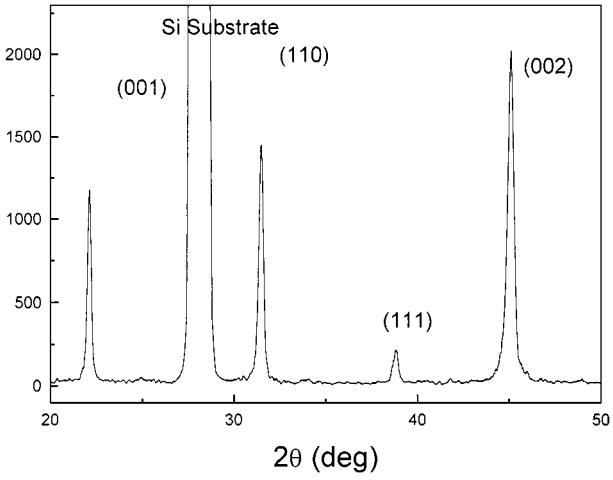

Figure 5 The X-ray θ-2θ scan patterns of the PFN films deposited on Si(100) substrates.

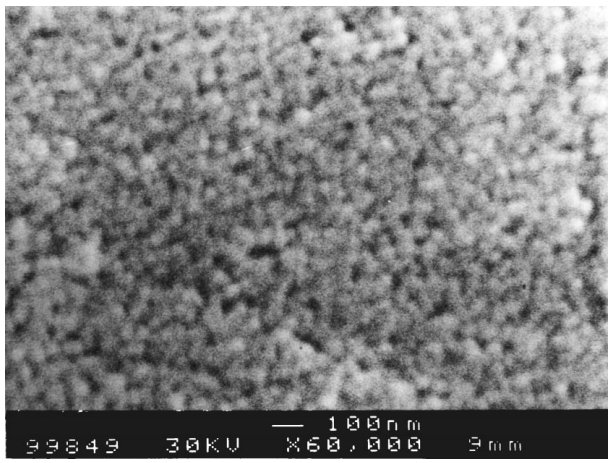

Figure 6 The scanning electron microscopy surface morphology of the PFN film.

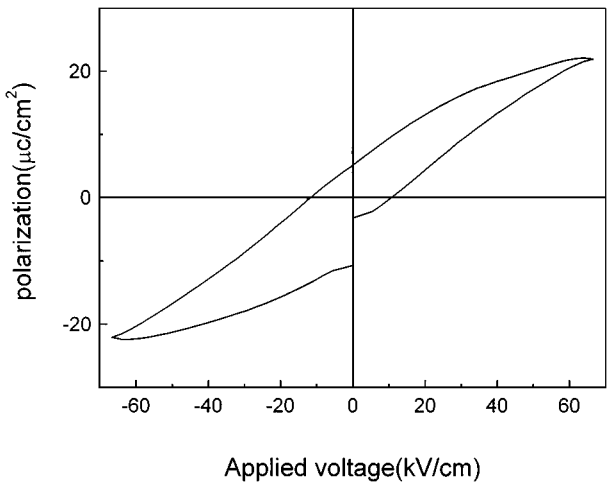

Figure 7 The Hysteresis loops of the PFN thin films (at an maximum applied voltage of 10 V, Pr = 7.4 μC/cm^2, Ec = 10.5 kV/cm).

samples, the remnant polarization of thin films is smaller than that of the former, whereas the coercive field becomes much larger. These may be related to the loss of PbO and the size effect of PFN thin films. The P-E hysteresis loop also shows asymmetry. It can be ascribed to the Schottky barrier exiting in the metal-oxide interface. The barrier introduces an internal electrical

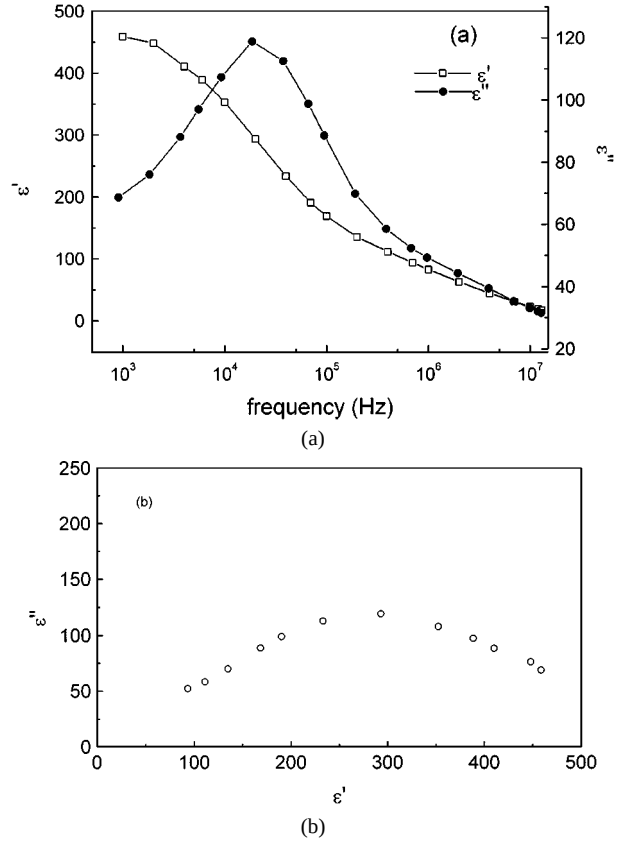

Figure 8 (a) The dielectric spectra of the PFN thin films (b) Cole-Cole plots of the PFN thin films. (c) The temperature dependence of the dielectric constant and the dissipation factor of PFN thin films.

field between the two electrodes. Therefore, an external bias field is needed to compensate the internal field [13]. Although the remnant polarization is about half of that of PFN bulk samples, it is still much larger than that previously reported [14], thus making it a possible candidate for application in non-volatile ferroelectric random access memory devices (FERAM).

Dielectric spectra of PFN thin films are presented in Fig. 8a. The dielectric properties of the PFN thin films are similar to that of bulk samples. They also exhibit the characteristics of the typical dielectric relaxation with a corresponding relaxation time of 3×10^{-5} s, different from that of the bulk sample. Cole-Cole plots of the PFN films are drawn in Fig. 8b. Unlike the bulk samples, the Cole-Cole plots of the thin films approximate to an arc indicating that their relaxation time spreads in a wide range. This is probably due to more complicated mechanisms. Fig. 8c is the temperature dependence of dielectric constant. We found that the peak of dielectric constant at the curie point of bulk PFN (at 380 K) can not be observed, but the curve of dissipation factor shows a broad peak at about 360 K which is similar to that of PFN bulk ceramic samples. At room temperature, the dielectric constant and the dissipation factor are 458 and 0.21 at 10 kHz, respectively. The dielectric constant is smaller than that of the corresponding bulk samples.

The curve of the leakage current versus applied electric field is shown in Fig. 9. It shows that there is a terrace at an applied field range from 40 kV/cm to 106 kV/cm, above which leakage current increases quickly. We suppose that the characteristics of the leakage current below the applied field of 106 kV/cm is mainly dominated

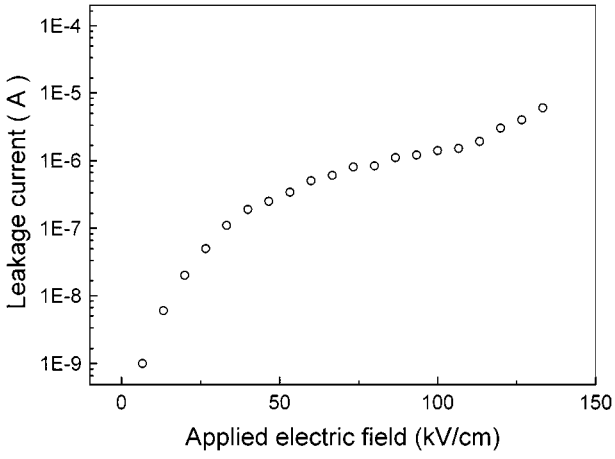

Figure 9 The leakage current characteristics of the PFN films.

by Schottky field emission, whereas in high electric field region they are dominated by Fowler-Nordheim tunneling [15].

4. Summary

Ferroelectromagnets PFN ceramics and thin films have been prepared by solid state reaction method and pulsed laser deposition technique, respectively. *P-E* hysterysis loop measurements showed that the remnant polarization of ceramics and thin films are 11.5 μC/cm^2 and 7.4 μC/cm^2 respectively. Temperature dependence of dielectric constant showed that the para-ferroelectric transition in PFN at 380 K is diffusive in character, which is caused by the redistribution of Fe^{3+} and Nb^{5+} ions in B site of ABO_3 compound. Anomalies in the dielectric properties have been observed near the para-antiferromagnetic transition temperature at about 145 K. The ferroelectric, dielectric, and leakage current properties of PFN films were also investigated. The result indicated that PFN films are potential materials for non-volatile ferrolectric memory and high dielectric constant DRAM applications.

Acknowledgement

The work was supported by a grant for State Key Program for Basic Research of China and the National Natural Science Foundation of China.

References

1. G. A. SMOLENSKII, A. I. AGRANOVSKYA, S. V. ISUPOV and V. A. ISUPOV, *Sov. Phys-Teach. Phys.* **3** (1958) 1981.
2. V. A. BOKOV, I. E. MYLNIKOV and G. A. SMOLENSKII, *Sov. Phys. JEPT.* **42** (1961) 643.
3. M. YOKOSUKA, *Jpn. J. Appl. Phys. Lett.* **32** (1993) 1142.
4. M. H. LEE and W. K. CHOO, *J. Alppl. Phys.* **52** (1981) 5767.
5. Q. LUO, X. Y. CHEN, Z. G. LIU, Z. M. SUN and N. B. MING, *Appl. Surf. Sci.* **108** (1997) 89.
6. G. A. SMOLENSKII, *J. Phys. Soc. Jpn.* **28** (1970) 26.
7. L. E. CROSS, S. JANG, R. E. NEWNHAM, S. NMURA and K. UCHINO, *Ferroelectrics* **23** (1980) 187.
8. J. F. SCOTT and D. R. TILLEY, *ibid.* **161** (1994) 235.
9. D. L. FOX, D. R. TILLEY, J. F. SCOTT and H. J. GUGGENHEIM, *Phys. Rev. B.* **21** (1980) 2926.
10. Z. J. HUNG, Y. CAO, Y. Y. SUN and C. W. CHU, *ibid.* **56** (1997) 2623.
11. K. S. COLE, K. H. COLE and A. J. BURAGGRAFF, *J. Am. Phys. Soc.* **51** (1980) 4956.
12. J. R. MACDONALD, *J. Chem. Phys.* **61** (1974) 3977.
13. K. KIM and C. SUDHUMA, *Mater. Res. Symp. Proc.* **265** (1992) 313.
14. X. R. WANG, S. S. FAN, Q. Q. LI, B. L. GU and X. W. ZHANG, **35** (1996) 1002.
15. J. F. SCOTT, M. AZUMA, E. FUJI, T. OTSUKI, G. KANNA, C. PAZDE ARAUJO, L. D. MCMILLAN and T. ROBERTS, Proc. ISAF'92 (1992) p. 356.

Received 24 June
and accepted 21 December 1999